Stochastic Modeling and Applications
Vol. 26. No. 1 (January-June, 2022)
ISSN: 0972-3641

Received: 16th February 2022 Revised: 09th April 2022 Selected: 30th April 2022

MATHEMATICAL MODELLING OF EXTERNAL BALLISTICS OF SLUGS WITH VARRYING PROPELLANT CHARGE EFFECTS

F.A. ZARGAR, H.A. BHAT, MUDASIR ASHRAF, AND VIVEK SHARMA

Abstract. This paper presents a mathematical model for the external ballistics of 12-gauge shotgun slugs that incorporates gravity, quadratic aerodynamic drag, and the influence of propellant charge via the muzzle velocity. We derive the governing equations from Newton's second law, provide closed vacuum solutions, obtain dimensionless forms that highlight key parameters (ballistic coefficient and drag number) and present numerical integration for realistic drag. We also include schematics of Foster and Brenneke slugs and simulated results: trajectory in vacuum and air (with drag), velocity decay, and range sensitivity to propellant charge. The model clarifies why slugs—with low ballistic coefficients—slow rapidly and have a short effective range, and how charge selection primarily acts through the initial velocity. Lastly, we discuss implications for hunting, law enforcement, and forensic reconstruction.

1. Introduction

Ballistics is the scientific study of the motion of projectiles and the forces that act on them. Traditionally, it is divided into three major domains - internal ballistics, intermediate ballistics, and external ballistics [6].

Internal ballistics refers to the processes inside the firearm prior to the exit of the projectile from the barrel. It includes ignition of the propellant, pressure buildup, acceleration of the projectile, and determination of the muzzle velocity. Intermediate ballistics is the short but complex transition phase as the projectile exits the muzzle. During this stage, expanding propellant gasses overtake the projectile, generating turbulence, muzzle blast, and shock waves that may induce yaw or instability[7, 1, 8]. Although it lasts only a few milliseconds, it plays a critical role in accuracy and dispersion. External ballistics studies projectile motion from muzzle exit to impact [10]. The trajectory of the projectile is affected by gravity, aerodynamic drag, wind, and atmospheric conditions. Unlike high-speed rifle bullets, shotgun slugs typically possess lower ballistic coefficients, leading to rapid velocity decay and a more curved trajectory.

Shotgun slugs differ from rifle bullets by that they have a larger diameter, a blunt shape, and a markedly lower ballistic coefficient (BC), resulting in rapid

2000 *Mathematics Subject Classification.* 03C74; 03C74-10.
Key words and phrases. Ballistics, slugs, shotgun, forensic ballistics, mathematical modelling.

deceleration and steep trajectories. Accurate modelling supports forensic reconstructions [11], sighting and zeroing decisions, and safe/ethical range estimates. In this paper we; (i) derive a practical model, (ii) quantify the effect of aerodynamic drag, and (iii) link the propellant charge to the external solution through the muzzle velocity v_0.

2. Slug Design and Characteristics

In this study we mathematically study the external ballistics of some common 12-gauge slugs such as Foster - hollow base, with external fins, Brenneke - solid slug with attached wad and Sabot - small high velocity slugs designed for rifled firearms [9, 5].

FIGURE 1. Depiction of various types of slugs.

Typical baseline values used for numerical simulations in this study are mass m = 28 g, diameter d = 18.5 mm, muzzle velocity $v_0 = 400$ m/s, and drag coefficient $C_d = 0.20$. The frontal area is $A = \pi(d/2)^2$. For the sake of this study, the form of *ballistic coefficient* [2] used is

$$BC = \frac{m}{C_d A}. \tag{2.1}$$

3. Governing Equations of Motion

3.1. Forces and Kinematics. After exiting the muzzle , the slug faces the effect of gravity and quadratic drag [4]. Incorporating these forces, we therefore have

$$\mathbf{F} = m\mathbf{a} = m\dot{\mathbf{v}} = m\begin{bmatrix}\dot{v}_x \\ \dot{v}_y\end{bmatrix}, \quad \mathbf{W} = \begin{bmatrix}0 \\ -mg\end{bmatrix}, \tag{3.1}$$

$$\mathbf{D} = -\tfrac{1}{2}\rho C_d A\, v\, \mathbf{v}, \quad v = \sqrt{v_x^2 + v_y^2}. \tag{3.2}$$

Hence the component equations are

$$m\dot{v}_x = -\tfrac{1}{2}\rho C_d A\, v\, v_x, \tag{3.3}$$

$$m\dot{v}_y = -mg - \tfrac{1}{2}\rho C_d A\, v\, v_y. \tag{3.4}$$

Position follows from $\dot{x} = v_x,\ \dot{y} = v_y$. Figure 2 illustrates the force model.

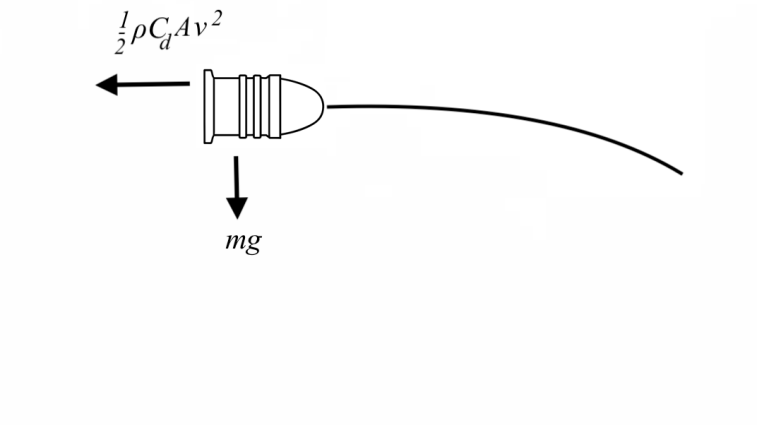

FIGURE 2. Forces on a slug in flight: weight mg and quadratic drag $\frac{1}{2}\rho C_d A v^2$ opposite to velocity.

3.2. Vacuum Reference (Closed Form). With $C_d = 0$, the classical solution for launch speed v_0 and angle θ is

$$x(t) = v_0 \cos\theta\, t, \tag{3.5}$$

$$y(t) = v_0 \sin\theta\, t - \tfrac{1}{2} g t^2. \tag{3.6}$$

It is useful as an upper bound on range of the slug.

3.3. Dimensionless Form. Let V be a characteristic speed (v_0), L the characteristic length ($L = V^2/g$), and define

$$\tilde{t} = \frac{tV}{L} = \frac{gt}{V}, \quad \tilde{v}_i = \frac{v_i}{V}, \quad \tilde{x} = \frac{x}{L},\ \tilde{y} = \frac{y}{L}.$$

Introduce the *drag number*

$$\Lambda \equiv \frac{\rho C_d A L}{2m} = \frac{\rho C_d A}{2m}\frac{V^2}{g} = \frac{V^2}{g}\frac{1}{2\,BC}, \tag{3.7}$$

where BC is from (2.1). Then (3.3)–(3.4) become

$$\frac{d\tilde{v}_x}{d\tilde{t}} = -\Lambda\, \tilde{v}\, \tilde{v}_x, \tag{3.8}$$

$$\frac{d\tilde{v}_y}{d\tilde{t}} = -1 - \Lambda\, \tilde{v}\, \tilde{v}_y, \tag{3.9}$$

with $\tilde{v} = \sqrt{\tilde{v}_x^2 + \tilde{v}_y^2}$. Thus, the shape of the trajectory of the slug after muzzle exit is governed by Λ (and hence hence BC) and launch conditions.

4. Effect of Propellant Charge manifested by Muzzle Velocity

Let M_c be propellant mass and Q its specific energy (J/kg). If η is the efficiency of converting chemical energy to kinetic energy [13] of the slug, accounted for gas work, thermal losses, and barrel friction, a practical relation between these parameters is

$$E_c = M_c Q, \qquad \frac{1}{2} m v_0^2 \approx \eta\, E_c, \tag{4.1}$$

which gives

$$v_0 = \sqrt{\frac{2\eta M_c Q}{m}}. \tag{4.2}$$

Typical shotgun propellants have $Q \sim (3.5\text{–}4.5) \times 10^6\ J/kg$; η is commonly $\sim$ 0.3–0.4 as an empirical lumped factor (accounting for barrel length, expansion ratio and other related factors). Equation (4.2) sets the initial condition

$$v_x(0) = v_0 \cos\theta, \qquad v_y(0) = v_0 \sin\theta, \tag{4.3}$$

which feeds the external solution dominated by drag (3.3)–(3.4).

5. Analytical Approximations

No general closed form solution to the model exists with quadratic drag, however, the following approximations provide useful insights:

5.1. Small-Angle, Flat-Fire Approximation. For θ a few degrees and a slight drop initially, the range R scales approximately as

$$R \approx \frac{2mv_0}{\rho C_d A g} = \frac{2\, BC\, v_0}{g}. \tag{5.1}$$

This shows linear dependence on v_0 (hence $\propto \sqrt{M_c}$) and on BC.

5.2. Early-Time Speed Decay. For the first fraction of a second when $v \approx v_0$, one may write $\dot{v} \approx -kv^2 - g\sin\phi$ with $k = (\rho C_d A)/(2m)$ and flight-path angle ϕ. Neglecting gravity along the track gives $v(t) \approx v_0/(1 + kv_0 t)$, explaing the strong quadratic-drag slowdown.

6. Numerical Method

We integrate (3.3)–(3.4) coupled with $\dot{x} = v_x, \dot{y} = v_y$ using a fixed-step fourth-order Runge–Kutta (RK4) [3] with atmospheric parameters $\rho = 1.2 kg/m^3$ at $\theta = 5^\circ$. Different C_d values were assigned to represent various types of slugs which along with the results obtained are given in Table 1.

TABLE 1. Numerical results for representative slug types

Slug Type	C_d	Range (m)	Flight Time (s)
Foster (low-BC)	0.25	930.3	4.919
Brenneke (mid-BC)	0.18	1079.6	4.999
Sabot (high-BC)	0.08	1412.7	4.999

7. Results and Discussion

7.1. Trajectories: Vacuum vs. Drag.

Vacuum vs. drag-influenced trajectories. As a reference, in the absence of aerodynamic drag ($k_i = 0$), the classical vacuum trajectory is [**?**]

$$x(t) = v_0 \cos\theta\, t, \tag{7.1}$$

$$y(t) = v_0 \sin\theta\, t - \tfrac{1}{2} g t^2, \tag{7.2}$$

which traces a parabola with analytic range

$$R_{\text{vac}} = \frac{v_0^2 \sin(2\theta)}{g}. \tag{7.3}$$

With quadratic drag ($k_i > 0$), the governing system becomes

$$\frac{dx}{dt} = v_x, \qquad \frac{dy}{dt} = v_y, \tag{7.4}$$

$$\frac{dv_x}{dt} = -k_i\, v\, v_x, \qquad \frac{dv_y}{dt} = -g - k_i\, v\, v_y, \tag{7.5}$$

which admits no closed form and is solved numerically. The deviation from the vacuum parabola increases with drag constant k_i, hence is most severe for the Foster slug, moderate for Brenneke, and least for the Sabot.

7.2. Slug-dependent drag constant and early-time velocity decay. For a given slug type, characterized by its drag coefficient C_d, define the drag constant

$$k \;\equiv\; \frac{\rho\, C_d\, A}{2m}, \tag{7.6}$$

and the ballistic coefficient

$$BC \;\equiv\; \frac{m}{C_d A}. \tag{7.7}$$

A convenient *characteristic decay time* and *length* are

$$\tau \;=\; \frac{1}{k\, v_0}, \qquad \ell \;=\; \frac{1}{k}. \tag{7.8}$$

Under the standard early-time approximation (gravity neglected along the velocity direction), the speed satisfies

$$\frac{dv}{dt} \;=\; -k\, v^2 \;\;\Longrightarrow\;\; v(t) \;=\; \frac{v_0}{1 + k\, v_0\, t}, \tag{7.9}$$

and the kinetic-energy retention obeys

$$\frac{E(t)}{E(0)} \;=\; \left(\frac{v(t)}{v_0}\right)^2 \;=\; \frac{1}{(1 + k\, v_0\, t)^2}. \tag{7.10}$$

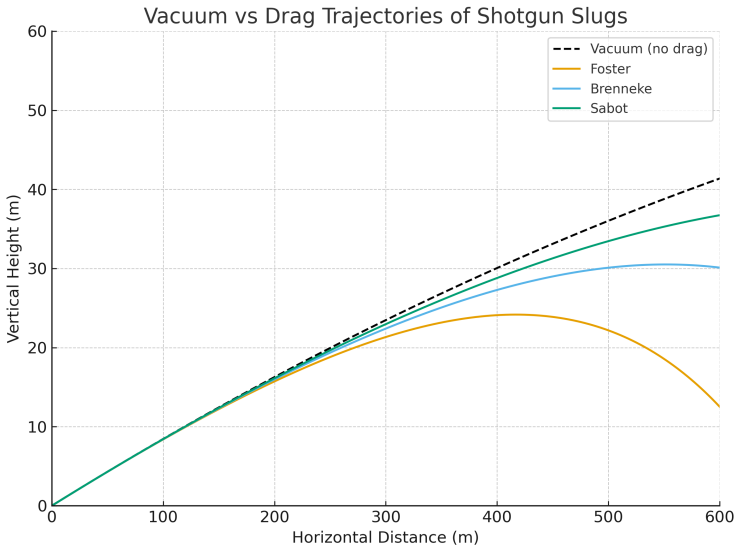

FIGURE 3. Comparison of the ideal vacuum parabola with drag-affected trajectories for Foster, Brenneke, and Sabot slugs at $v_0 = 400$ m/s and $\theta = 5°$.

For small launch angles, a useful horizontal-displacement approximation is

$$x(t) \approx \frac{\cos\theta}{k} \ln\bigl(1 + k\, v_0\, t\bigr), \tag{7.11}$$

illustrating explicitly how *slug type* (via C_d and thus k and BC) controls deceleration and downrange progression.

TABLE 2. Velocity and mpact data for slug types with baseline parameters.

Slug	C_d	k (1/m)	$v(0)$	$v(0.1s)$	$v(0.5s)$	$v(1.0s)$	Time (s)	Speed (m/s)
Foster	0.25	1.440×10^{-3}	399.9	351.5	220.9	147.3	4.919	174.537
Brenneke	0.18	1.037×10^{-3}	399.9	362.1	254.6	179.6	4.999	197.301
Sabot	0.08	4.608×10^{-4}	399.9	372.8	298.9	230.9	4.999	271.527

7.3. Effect of Propellant Charge. The effect of varying propellant charge was investigated by considering three muzzle velocities, $v_0 = 350, 400$, and 450 m/s, for the Foster, Brenneke, and Sabot slugs. An increase in propellant charge translates directly into a higher muzzle velocity [12, 13], which in turn alters the velocity decay, range, and downrange impact energy of the projectile. While the qualitative trend is consistent across all slug types, the magnitude of improvement is strongly dependent on the ballistic coefficient (BC).

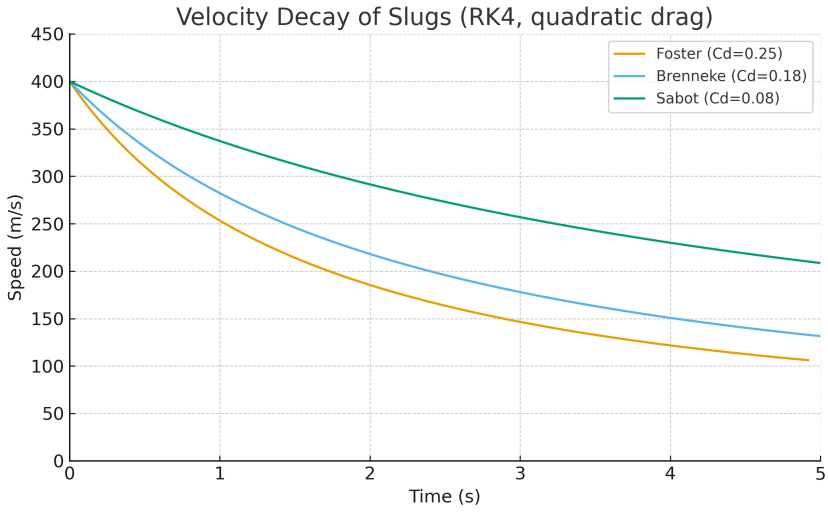

FIGURE 4. Velocity decay under quadratic drag (same parameters as Fig. 3).

Table 3 shows the calculated impact speeds at a fixed downrange distance of 100 m. For all slug types, the impact speed increases with muzzle velocity. However, because of differing aerodynamic efficiencies, the absolute gains differ: the Sabot slug with highest BC retains the greatest fraction of its muzzle energy, while the Foster slug with lowest BC loses velocity more rapidly.

TABLE 3. Impact speed at 100 m for various muzzle velocities v_0 and slug types.

Slug Type	$v_0 = 350$ m/s	$v_0 = 400$ m/s	$v_0 = 450$ m/s
Foster	302.68	345.97	389.26
Brenneke	315.18	360.26	405.34
Sabot	333.95	381.72	429.48

Table 4 presents the results of full trajectory simulations, reporting the maximum range (horizontal distance until ground impact) and final ground-impact speed. The Foster slug shows limited benefit from increased charge because of its high drag; in fact, the ground-impact speed slightly decreases as v_0 increases, due to longer flight time and energy lost to drag. In contrast, the Brenneke slug demonstrates moderate gains, and the Sabot slug benefits substantially in both the range and retained impact velocity.

The graphical comparison further illustrates these differences. Figure 5 shows the impact speed at 100 m as a function of muzzle velocity, while Figure 6 depicts the corresponding variation in total range. Both plots highlight the superior performance of the Sabot slug, where increases in propellant charge translate almost linearly into greater downrange performance. This confirms that while higher

TABLE 4. Range (m) and ground-impact speed (m/s) from full-flight simulation for each slug type and v_0.

Slug / v_0	Range (m)	Impact speed (m/s)
Foster, 350 m/s	825.87	107.63
Foster, 400 m/s	930.38	106.08
Foster, 450 m/s	1024.89	104.41
Brenneke, 350 m/s	975.75	128.20
Brenneke, 400 m/s	1114.22	127.17
Brenneke, 450 m/s	1241.04	125.70
Sabot, 350 m/s	1361.79	187.54
Sabot, 400 m/s	1614.35	190.98
Sabot, 450 m/s	1856.09	192.43

charge does provide additional energy, the projectile's aerodynamic design (and thus BC) plays the dominant role in determining retained velocity and effective range.

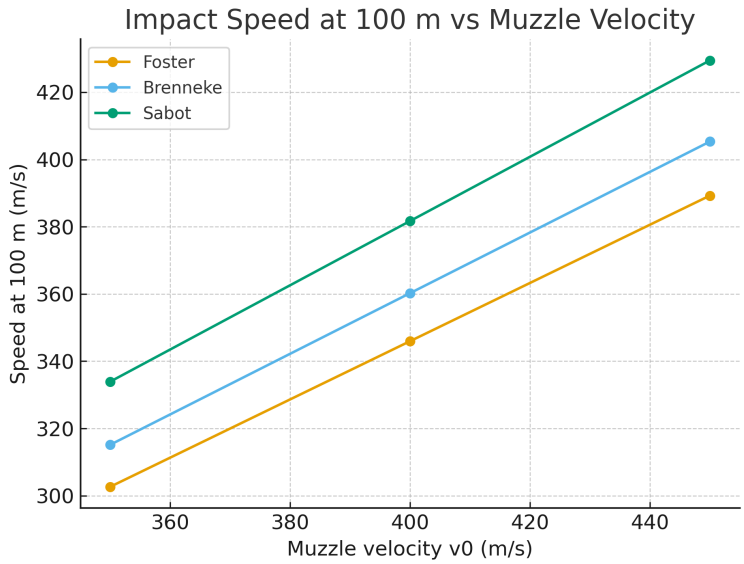

FIGURE 5. Impact speed at 100 m versus muzzle velocity v_0 for Foster, Brenneke and Sabot slugs.

In summary, increased propellant charge does raise downrange performance for all slug types, but the relative benefit depends critically on slug aerodynamics. From an applied ballistics perspective, improving projectile design (BC) is often more effective than relying solely on increased propellant charge, especially given chamber pressure and recoil constraints.

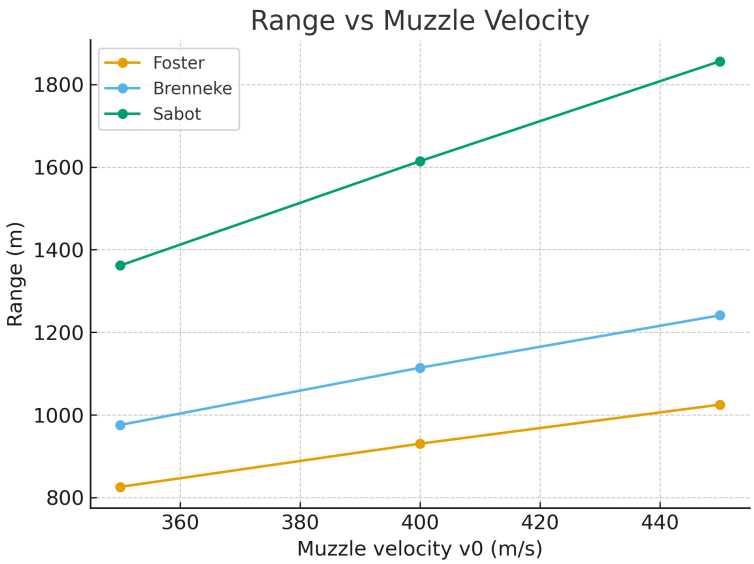

FIGURE 6. Range vs Muzzle velocity v_0 for Foster, Brenneke and Sabot slugs.

8. Conclusions

We have presented a compact model connecting propellant charge to external ballistics through the muzzle velocity, then propagating motion with gravity and quadratic drag. Dimensionless analysis shows the dependence of external ballistics on BC (geometry & mass) and a drag number. Simulations quantify why slugs with low BC have short effective ranges and strong early deceleration, and show how charge selection primarily acts by increasing v_0. Extensions may include wind, yaw-drag coupling, spin/fin stabilization, and temperature/altitude effects on ρ.

Furthermore, the findings of this study carry significant practical implications. The study highlights the importance of maintaining consistent propellant charges to ensure ethical energy transfer, predictable trajectories, and reduced risk of over-penetration in ethical hunting practices. This study also finds applications in law-enforcement as the sensitivity of slug performance to propellant variations underscores the need for strict ammunition standardization to guarantee reliable precision, barrier-penetration characteristics, and operational safety. In forensic reconstruction, the presented ballistic equations and sensitivity analysis offer a robust framework for estimating firing distance, projectile energy, and slug type in cases involving altered or reloaded ammunition. Thus, the developed model not only advances theoretical understanding of external ballistics but also enhances practical decision-making in real-world civilian, tactical, and forensic environments.

References

1. Bryan L.: *Aerodynamic Drag Modeling for Ballistics*, Applied Ballistics, 2021.
2. Crawford K., Mitiukov N. , Busygina E. and Alies M.: *Internal ballistics of smoothbore guns*, IOP Conference Series: Materials Science and Engineering **971** (2020).
3. Evans D.: *A new 4th order runge-kutta method for initial value problems with error control*, International Journal of Computer Mathematics **39** 1991.
4. Di Maio V.: *Gunshot Wounds: Practical Aspects of Firearms, Ballistics, and Forensic Techniques*, CRC Press 2015.
5. Donald E., Carlucci S., Jacobson S.: *Ballistics: Theory and Design of Guns and Ammunition*, CRC Press 2018.
6. Heard B.J.: *Handbook of Firearms and Ballistics* 2nd ed, Wiley 2008.
7. Jang, Jin-Sung, et al: *Numerical study on properties of interior ballistics according to solid propellant position in chamber*, Fluids Engineering Division Summer Meeting **44403** (2011).
8. Krcmar, Jan, Claude S., Khalid D.: *Interior ballistics simulation of the two chambers GLMAV launcher*. Propellants, Explosives, Pyrotechnics **39** (2014).
9. Lucas A., O.B.E., F.I.C.: *The examination of firearms and projectiles in forensic cases*, Analyst **566** (1923).
10. McCoy R.L.: *Modern Exterior Ballistics: The Launch and Flight Dynamics of Symmetric Projectiles*, Schiffer 2012.
11. Mattijssen E., Kerkhoff W.: *Bullet trajectory reconstruction – Methods, accuracy and precision*, Forensic Science International **262** (2016), 204-211.
12. Pejsa J.: *Modern Practical Ballistics*, Pejsa Ballistics Publications 2004.
13. Rashad M., Zhang X., Elsadek H.: *Interior ballistic two-phase flow model of guided-projectile gun system utilizing stick propellant charge*, Propellants, Explosives, Pyrotechnics 2014.

F.A ZARGAR: Sher-i-Kashmir Institute of Medical Sciences, Srinagar, India - 190011
Email address: faizanzgr@gmail.com

H.A. BHAT: Department of Electronics & Instrumentation Technology, Kashmir University, Srinagar, India - 190020
Email address: hilalbhat25@gmail.com

MUDASIR ASHRAF: Sher-i-Kashmir Institute of Medical Sciences, Srinagar, India - 190011
Email address: mudasirashraf9@gmail.com

VIVEK SHARMA: Sherlock Institute of Forensic Sciences, New Delhi, India - 110033
Email address: viveksharma110799@gmail.com